

<https://helda.helsinki.fi>

---

## Long-term dynamics of soil, tree stem and ecosystem methane fluxes in a riparian forest

Mander, Ülo

2022-02-25

---

Mander, Ü, Krasnova, A, Schindler, T, Megonigal, J P, Escuer-Gatius, J, Espenberg, M, Machacova, K, Maddison, M, Pärn, J, Ranniku, R, Pihlatie, M, Kasak, K, Niinemets, Ü & Soosaar, K 2022, ' Long-term dynamics of soil, tree stem and ecosystem methane fluxes in a riparian forest ', Science of the Total Environment , vol. 809 , 151723 . <https://doi.org/10.1016/j.scitotenv.2021.151723>

---

<http://hdl.handle.net/10138/352805>

<https://doi.org/10.1016/j.scitotenv.2021.151723>

---

cc\_by\_nc\_nd

acceptedVersion

---

*Downloaded from Helda, University of Helsinki institutional repository.*

*This is an electronic reprint of the original article.*

*This reprint may differ from the original in pagination and typographic detail.*

*Please cite the original version.*



Contents lists available at ScienceDirect

Science of the Total Environment

journal homepage: [www.elsevier.com/locate/scitotenv](http://www.elsevier.com/locate/scitotenv)

## Long-term dynamics of soil, tree stem and ecosystem methane fluxes in a riparian forest

Ülo Mander<sup>a,b,\*</sup>, Alisa Krasnova<sup>a,c</sup>, Thomas Schindler<sup>a,b</sup>, J. Patrick Megonigal<sup>d</sup>, Jordi Escuer-Gatius<sup>e</sup>, Mikko Espenberg<sup>a</sup>, Katerina Machacova<sup>a,b</sup>, Martin Maddison<sup>a</sup>, Jaan Pärn<sup>a</sup>, Reti Ranniku<sup>a</sup>, Mari Pihlatie<sup>f,g,h</sup>, Kuno Kasak<sup>a</sup>, Ülo Niinemets<sup>e</sup>, Kaido Soosaar<sup>a,b</sup>

<sup>a</sup> Department of Geography, Institute of Ecology & Earth Sciences, University of Tartu, Vanemuise 46, 51014 Tartu, Estonia

<sup>b</sup> Global Change Research Institute of the Czech Academy of Sciences, Department of Ecosystem Trace Gas Exchange, Belidla 986/4a, 603 00 Brno, Czech Republic

<sup>c</sup> Institute of Forestry and Rural Engineering, Estonian University of Life Sciences, Kreutzwaldi 1, 51006 Tartu, Estonia

<sup>d</sup> Smithsonian Environmental Institute, 647 Contees Wharf Road Edgewater, MD 21037-0028, USA

<sup>e</sup> Institute of Agricultural & Environmental Sciences, Estonian University of Life Sciences, Kreutzwaldi 5, 51006 Tartu, Estonia

<sup>f</sup> Department of Agricultural Sciences, Environmental Soil Sciences, University of Helsinki, Latokartanonkaari 7, 00014 Helsinki, Finland

<sup>g</sup> Institute for Atmospheric and Earth System Research (INAR) / Forest Science, University of Helsinki, Physicum, Kumpula campus, Gustaf Hällströmin katu 2, 00560 Helsinki, Finland

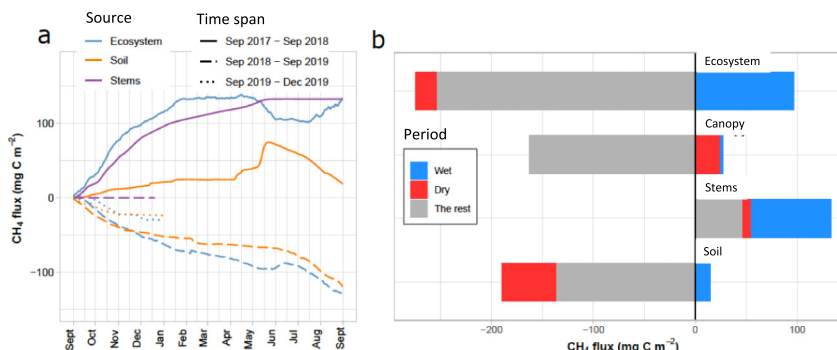
<sup>h</sup> Department of Agricultural Sciences, Viikki Plant Science Centre (ViPS), University of Helsinki, Viikinkaari 2a, 00014 Helsinki, Finland

### HIGHLIGHTS

- Significant difference in CH<sub>4</sub> fluxes between the wet and dry periods
- Wet period: 83% of ecosystem CH<sub>4</sub> emission moves through the tree stems
- Dry period: CH<sub>4</sub> consumed in the soil and emitted from the canopy
- Strong positive correlation of soil and stem CH<sub>4</sub> fluxes with soil water content
- In a long term, riparian alder forests constitute a minor CH<sub>4</sub> sink

### GRAPHICAL ABSTRACT

During the 2.5-yr study the forest was a CH<sub>4</sub> sink. However, in the wet period (Sep-Dec 2017) 83% of CH<sub>4</sub> was emitted from the tree stems whereas in the dry period CH<sub>4</sub> was consumed in the soil and stem emission was very low.



### ARTICLE INFO

#### Article history:

Received 15 September 2021

Received in revised form 20 October 2021

Accepted 12 November 2021

Available online xxx

Editor: Pavlos Kassomenos

#### Keywords:

Automated chambers

Eddy covariance

Quantum cascade laser absorption

### ABSTRACT

The carbon (C) budgets of riparian forests are sensitive to climatic variability. Therefore, riparian forests are hot spots of C cycling in landscapes. Only a limited number of studies on continuous measurements of methane (CH<sub>4</sub>) fluxes from riparian forests is available. Here, we report continuous high-frequency soil and ecosystem (eddy-covariance; EC) measurements of CH<sub>4</sub> fluxes with a quantum cascade laser absorption spectrometer for a 2.5-year period and measurements of CH<sub>4</sub> fluxes from tree stems using manual chambers for a 1.5 year period from a temperate riparian *Alnus incana* forest.

The results demonstrate that the riparian forest is a minor net annual sink of CH<sub>4</sub> consuming 0.24 kg CH<sub>4</sub>-C ha<sup>-1</sup> y<sup>-1</sup>. Soil water content is the most important determinant of soil, stem, and EC fluxes, followed by soil temperature. There were significant differences in CH<sub>4</sub> fluxes between the wet and dry periods. During the wet period, 83% of CH<sub>4</sub> was emitted from the tree stems while the ecosystem-level emission was equal to the sum of soil and stem emissions. During the dry period, CH<sub>4</sub> was substantially consumed in the soil whereas stem emissions were very

\* Corresponding author at: Department of Geography, Institute of Ecology & Earth Sciences, University of Tartu, Vanemuise 46, 51014 Tartu, Estonia.

E-mail address: [ulo.mander@ut.ee](mailto:ulo.mander@ut.ee) (Ü. Mander).

spectrometer  
Soil fluxes  
Soil water content  
Stem fluxes

low. A significant difference between the EC fluxes and the sum of soil and stem fluxes during the dry period is most likely caused by emission from the canopy whereas at the ecosystem level the forest was a clear CH<sub>4</sub> sink. Our results together with past measurements of CH<sub>4</sub> fluxes in other riparian forests suggest that temperate riparian forests can be long-term CH<sub>4</sub> sinks.

© 2021 Elsevier B.V. All rights reserved.

## 1. Introduction

Methane (CH<sub>4</sub>) is a greenhouse gas (GHG) with a global warming potential 28 to 45 times that of carbon dioxide (CO<sub>2</sub>) (IPCC, 2014; Neubauer and Megonigal, 2015). Atmospheric CH<sub>4</sub> is responsible for approximately 20% of global warming since the preindustrial era (Kirschke et al., 2013). In ecosystems, CH<sub>4</sub> is primarily produced in anaerobic environments by methanogens and oxidised to CO<sub>2</sub> in aerobic environments by methanotrophs (Megonigal et al., 2004).

Forests are the most important ecosystems in the global terrestrial carbon cycle, maintaining 86% of the standing plant carbon (C) pool and 73% of the soil C pool (Pan et al., 2011). Upland forest soils are dominant terrestrial components in the global CH<sub>4</sub> budget as a sink of atmospheric CH<sub>4</sub> (Dutaur and Verchot, 2007; Dlugokencky et al., 2011; Saunois et al., 2020). Of the total CH<sub>4</sub> consumed in soils at the global scale, 60% corresponds to forest ecosystems with the yearly uptake estimated at 9.16 Tg CH<sub>4</sub> y<sup>-1</sup> (Dutaur and Verchot, 2007; Yu et al., 2017). However, because of the joint effects of climate change and land-use changes, a decline in soil CH<sub>4</sub> uptake has been identified in forests across the globe (Ni and Groffman, 2018; Han and Zhu, 2020). On the other hand, wetland forest soils are significant CH<sub>4</sub> sources (Salm et al., 2012; Turetsky et al., 2014; Covey and Megonigal, 2019). Drainage can turn wetland forest soils from sources to sinks (Minkinen et al., 2007; Ojanen et al., 2010; Abdalla et al., 2016; Viru et al., 2020; Carter et al., 2012; Tan et al., 2020), although this is not always the case (Petrescu et al., 2015). Large emissions have been measured from the soils of tropical wetland forests (Sakabe et al., 2018; Wong et al., 2018; Dalmagro et al., 2019; Griffis et al., 2020; Liu et al., 2020).

Forest CH<sub>4</sub> fluxes are the net balance of production, oxidation and transport of CH<sub>4</sub> through the ecosystem (Saunois et al., 2016; Covey and Megonigal, 2019; Flanagan et al., 2020). Methane may be produced in anaerobic soil layers and transported by trees to the atmosphere by several mechanisms including diffusion (Pangala et al., 2014; Megonigal et al., 2019), pressurized ventilation (Große and Schröder, 1984; Schröder, 1989), and mass flow as a solute in the transpiration stream to the atmosphere (Covey and Megonigal, 2019). These transport mechanisms create a bypass for CH<sub>4</sub> avoiding its oxidation that may occur in upper layer of soils during diffusion of methane through the soil columns (Maier et al., 2018). In addition to plants acting as conduits for methane produced in soil substrates, methane can be directly produced in situ in some tree stems (Zeikus and Ward, 1974; Barba et al., 2019; Yip et al., 2019; Barba et al., 2021). Emission of methane from living tree stems in upland forests can be of the same magnitude as the methane sink in soils for brief periods of time (Pitz and Megonigal, 2017) or an annual basis (Wang et al., 2017), offsetting a portion of the soil CH<sub>4</sub> sink capacity of these ecosystems (Rice et al., 2010; Covey et al., 2012). Yet, CH<sub>4</sub> consumption by soils is the only process that has been regularly included in methane budgets for upland forest ecosystems (Saunois et al., 2016; Warner et al., 2017; Covey and Megonigal, 2019). Accounting for tree emissions can dramatically increase estimates of the amount of CH<sub>4</sub> emitted by forested wetlands (Pangala et al., 2013, 2015; Liu et al., 2020).

Numerous studies have considered methane fluxes from soils and tree stems in upland forests (Pitz and Megonigal, 2017; Warner et al., 2017; Barba et al., 2018; Maier et al., 2018; Covey and Megonigal,

2019; Machacova et al., 2021), and wetland and floodplain forests (Gauci et al., 2010; Pangala et al., 2013, 2015, 2017; Terazawa et al., 2015; Moldaschl et al., 2021), whereas a limited number of investigations have focused on riparian forests (Flanagan et al., 2020; Schindler et al., 2020). Riparian forests provide important ecosystem services (Riis et al., 2020) such a provisioning of water quality (Sweeney et al., 2004; Mander et al., 2017), and GHG regulation (Flanagan et al., 2020; Schindler et al., 2020). Grey alder (*Alnus incana* (L.) Moench.) forests are widely distributed in Europe and North America (Caudullo et al., 2017), often dominating riparian zones (Clerici et al., 2013). In Europe the area covered by *Alnus incana* subsp. *incana* forests reaches 15,000 km<sup>2</sup> (Caudullo et al., 2017). This is one reason why several tree-stem scale CH<sub>4</sub> studies have focused on *Alnus* species (Gauci et al., 2010; Machacova et al., 2013; Pangala et al., 2014; Schindler et al., 2020; Köhn et al., 2021).

Most studies of CH<sub>4</sub> emission and consumption by trees have focused on the main tree stem, however some studies report emission from shoots and leaves (Machacova et al., 2016). Ecosystem-level studies using the eddy covariance (EC) technique suggest that tree canopies contribute to the ecosystem CH<sub>4</sub> budget (do Carmo et al., 2006). Eddy covariance measurements of CH<sub>4</sub> fluxes have been conducted in boreal forests (Iwata et al., 2015; Nakai et al., 2020), temperate forests (Wang et al., 2013; Hommeltenberg et al., 2014; Shoemaker et al., 2014; Flanagan et al., 2020), and tropical/sub-tropical forests (do Carmo et al., 2006; Dalmagro et al., 2019; Griffis et al., 2020; Liu et al., 2020). In addition, data are available from FLUXNET network sites in Finland, Switzerland, Russia and Indonesia. The temperate and boreal EC stations are present both in upland and wetland forests whereas the tropical EC stations are mostly located in wetland forests. However, most previous studies did not separate soil versus tree stem sources or sinks which is needed to understand and model CH<sub>4</sub> cycling processes in forests. Thus, there is a gap in the forest CH<sub>4</sub> literature between whole-ecosystem (EC) studies that do not partition fluxes between soils and tree surfaces, and bottom-up studies that measure tree stems but not canopies.

Scaling and modelling forest CH<sub>4</sub> dynamics requires an understanding of the key environmental drivers of variability. It is well established that soil moisture is a primary determinant of CH<sub>4</sub> fluxes in both forest soils (negative relationship) and wetland soils (positive relationship) (Del Grosso et al., 2000; Smith et al., 2000; Dutaur and Verchot, 2007; Jungkunst et al., 2008; Shoemaker et al., 2014; Sakabe et al., 2018). There is evidence that soil moisture has similar effects on CH<sub>4</sub> fluxes across tree stems (Pitz et al., 2018; Barba et al., 2019; Schindler et al., 2020) and at the ecosystem-level (Hommeltenberg et al., 2014; Iwata et al., 2015; Wong et al., 2018; Nakai et al., 2020). The effects of soil moisture interact with temperature, which generally increases CH<sub>4</sub> fluxes, to determine the spatial and temporal patterns of CH<sub>4</sub> fluxes from forest soils (Itoh et al., 2008; Courtois et al., 2018) and tree stems (Vargas and Barba, 2019; Covey and Megonigal, 2019).

This paper aimed to analyse long-term ecosystem exchange of CH<sub>4</sub>, partition CH<sub>4</sub> exchanges between soils and tree stems, and relate CH<sub>4</sub> fluxes to key environmental factors in a representative temperate riparian grey alder forest. In particular, we sought to separate the contributions of tree stems and soil to overall ecosystem CH<sub>4</sub> fluxes. The second objective was to establish the factors responsible for temporal variations in CH<sub>4</sub> fluxes, in particular the impacts of

variation in soil-moisture and temperature. We tested the following hypotheses: (1) this riparian forest ecosystem is a net CH<sub>4</sub> sink, (2) ecosystem level (EC) CH<sub>4</sub> fluxes are equal to the sum of soil and stem fluxes, (3) soil moisture dynamics determine the long-term pattern of CH<sub>4</sub> fluxes, and (4) the tree stems are a bypass of soil CH<sub>4</sub> emissions i.e., we assume the stem emissions are positively correlated with soil emissions.

## 2. Material and methods

### 2.1. Study site description and location of eddy tower and soil chambers

The studied riparian forest is a 40-year *Filipendula* type grey alder (*A. incana* (L.) Moench) stand grown on former agricultural land (Fig. 1). It is situated in the Agali hamlet (58°17' N; 27°17' E) in eastern Estonia in the Lake Peipsi Lowland (Varep, 1964).

The area is characterised by flat relief with an average elevation of 32 m a.s.l., formed in the bottom of former periglacial lake systems. It is slightly inclined (1% slope) towards a tributary of the Kalli River. The soil is Gleyic Luvisol. The thickness of the humus layer was 15–20 cm. The content of total carbon (TC), total nitrogen (TN), Ca and Mg per dry matter in 10 cm topsoil was 2.42, 2.89, 1487 and 283 mg kg<sup>-1</sup>, respectively. This translated to a TC and TN contents of 3.8% and 0.33%, respectively. The abundance of these elements decreased precipitously below 20 cm dropping by 2–8 times in concentration (Supplementary Table 1).

The average annual precipitation of the region during the last 30 years is 650 mm (Kupper et al., 2011). Average annual air temperature is 5.8 °C whereas in July and January the mean air temperatures are 17.0 °C and – 6.7 °C, respectively. The duration of the growing season is typically 175–180 days from mid-April to October (Kupper et al., 2011).

The mean height of the forest stand is 17.5 m, the mean stem diameter at breast height is 15.6 cm and the growing stock is 245 m<sup>3</sup> ha<sup>-1</sup> (based on Uri et al. (2014) and Becker et al. (2015)). In the forest floor, the following herbs dominate: *Filipendula ulmaria* (L.) Maxim., *Aegopodium podagraria* L., *Cirsium oleraceum* (L.) Scop., *Geum rivale* L., *Crepis paludosa* (L.) Moench, shrubs (*Rubus idaeus* L., *Frangula alnus* L., *Daphne mezereum* L.) and young trees (*A. incana*, *Prunus padus* L.) dominate. In the moss-layer *Climacium dendroides* (Hedw.) F. Weber & D. Mohr, *Plagiomnium* spp. and *Rhytidiadelphus triquetrus* (Hedw.) Warnst. are common.

### 2.2. Soil flux measurements

Soil fluxes were measured using 12 automatic dynamic chambers located close to each studied tree and installed in June 2017. The chambers were made from polymethyl methacrylate (Plexiglas) covered with non-transparent plastic film. Each soil chamber (volume of 0.032 m<sup>3</sup>) covered a 0.16 m<sup>2</sup> soil surface. To avoid stratification of gas inside the chamber, air with a constant flow rate of 1.8 L min<sup>-1</sup> was circulated within a closed loop between the chamber and gas analyser unit during the measurements by a diaphragm pump. The air sample was taken from the top of the chamber headspace. For the measurements, each soil chamber was closed automatically for 9 min. Flushing time of the whole system with ambient air between measurement periods was 1 min. Thus, there were approximately 12 measurements per chamber per day. A Picarro G2508 (Picarro Inc., Santa Clara, CA, USA) gas analyser using cavity ring-down spectroscopy (CRDS) technology was used to monitor CH<sub>4</sub> gas concentrations at a frequency of approximately 1.17 Hz. The chambers were connected to the gas analyser using a multiplexer.

The whole 9 min period of chamber closure consisted of an initial 2 min period for stabilization of the trend. Thus, only 5 min of the linear trend of CH<sub>4</sub> concentration change was used for soil flux calculations. After the quality check we were able to use 105,500 (98% of total possible) of the soil CH<sub>4</sub> fluxes collected during the whole study period. Although plants were inside the chambers, we prefer to use the term “soil fluxes” instead of “floor fluxes”.

### 2.3. Stem flux measurements

The tree stem fluxes were measured manually with a frequency of once per week from September 2017 until December 2018. Twelve representative mature grey alder trees were selected for stem flux measurements and equipped with static closed tree stem chamber systems for stem flux measurements (Machacova et al., 2017). The tree chambers were installed in June 2017 on tree stems at approximately 10, 80 and 170 cm above the ground. The rectangular shaped stem chambers were made of transparent plastic containers, including removable airtight lids (Lock & Lock Co Ltd., Seoul, Republic of Korea). For chamber preparation see Machacova et al. (2017) and Schindler et al. (2020). Two chambers per each measurement height on tree stem were set randomly across 180° and interconnected with tubes into one system (total volume of 0.00119 m<sup>3</sup>) covering 0.0108 m<sup>2</sup> of



Fig. 1. Location and research set-up of the riparian grey alder forest in Agali, Estonia. Automated soil chambers, eddy tower and its footprint area are shown. Illustrations on the instrumental setup are presented in Supplementary Fig. 1.

stem surface. A pump (model 1410VD, 12 V; Thomas GmbH, Fürstenfeldbruck, Germany) was used to homogenize the gas concentration in paired chambers prior to sampling. Chamber systems remained open between each sampling campaign. During 60 measurement campaigns, four gas samples (each 25 mL) were collected from each chamber system via a septum at 60 min intervals in a sequence of 0/60/120/180 min and stored in pre-evacuated (0.3 bar) 12 mL gas-tight vials coated with pierceable chlorobutyl septum (LabCo International, Ceredigion, UK). In 16 campaigns both daytime (between 12:00 and 16:00) and nighttime (00:00–04:00) samples were taken. The gas samples were analysed in the laboratory at University of Tartu within a week using a gas chromatograph (GC-2014; Shimadzu, Kyoto, Japan) equipped with a flame ionization detector for CH<sub>4</sub>. The gas samples were injected automatically using Loftfield autosampler (Loftfield Analytics, Göttingen, Germany). For gas-chromatographical settings see Soosaar et al. (2011).

#### 2.4. Soil and stem flux calculations

Changes in CH<sub>4</sub> concentration in the chamber headspace over time were used to quantify the stem and soil fluxes as quantified by the linear approach of Livingston and Hutchinson (2015). A data quality control for the stem flux values was applied based on R<sup>2</sup> values of linear fit for CO<sub>2</sub> measurements. When R<sup>2</sup> of CO<sub>2</sub> efflux was >0.9, the CH<sub>4</sub> fluxes were used regardless of their R<sup>2</sup> values.

To compare the contribution of the soil and stems, the stem fluxes were upscaled to m<sup>2</sup> of ground area based on average stem diameter, tree height, stem surface area, tree density, and stand basal area. A cylindrical shape of tree stem was assumed. To estimate average stem emissions per tree, non-linear regression curves were fit between stem emissions and height for each measurement campaign as previously done by Schindler et al. (2020).

#### 2.5. Eddy covariance instrumentation

The eddy-covariance system was installed on a 21 m high scaffolding tower. A fast 3-D sonic anemometer Gill HS-50 (Gill Instruments Ltd., Lymington, Hampshire, UK) was used to obtain three wind components. Air was sampled with the 30 m Teflon inlet tube and analysed by a quantum cascade laser absorption spectrometer (QCLAS) (Aerodyne Research Inc., Billerica, MA, USA) for CH<sub>4</sub> concentrations. The QCLAS was installed in a heated and ventilated cottage near the tower base. A high-capacity free scroll vacuum pump (Agilent, Santa Clara, CA, USA) guaranteed air flow rate of 15 L min<sup>-1</sup> between the tower and QCLAS gas analyser during the measurements. Air was filtered for dust and condensed water. All measurements were done at 10 Hz and the QCLAS reported concentrations per dry air (mixing ratios).

#### 2.6. Eddy-covariance flux calculation and data quality control

The fluxes of CH<sub>4</sub> were calculated using the EddyPro software (v.6.0–7.0, Li-Cor) as a covariance of the gas mixing ratio with the vertical wind component over 30-min periods. De-spiking of the raw data was performed following Mauder et al. (2013). Anemometer tilt was corrected with the double axis rotation. Linear detrending was chosen over block averaging to minimize the influence of a possible fluctuations of a gas analyser. Time lags were detected using covariance maximisation in each time window (5 ± 2 s was chosen based on the tube length and flow rate). The water vapor correction was performed by the Aerodyne TDLWintel software, which reported mixing ratios. Both low and high frequency spectral corrections were applied using fully analytic corrections (Moncrieff et al., 1997, 2004).

Calculated fluxes were filtered out in case they were coming from the half-hour averaging periods with at least one of the following criteria: more than 1000 spikes, half-hourly averaged mixing ratio out

of range (1.8–2.5 ppm), quality control (QC) flags higher than 7 (Foken et al., 2004).

Footprint area was estimated using Kljun et al. (2015) implemented in TOVI software (Li-Cor Inc.). Footprint allocation tool was implemented to flag the non-forested areas within the 90% cumulative footprint and fluxes appointed to these areas were removed from the further analysis.

Storage fluxes were estimated using point concentration measurements from the eddy system, assuming the uniform change within the air column under the tower during every 30 min period (calculated in EddyPro software). In the absence of a better estimate or profile measurements, these estimates were used to correct for storage change. Friction velocity threshold of 0.29 ms<sup>-1</sup> was applied to eliminate low air mixing periods from the analysis (Papale et al., 2006). Total flux values that were higher than eight times the standard deviation were additionally filtered out (following Wang et al. (2013)). Overall, the quality control procedures resulted in 61% data coverage.

To obtain the continuous time-series and to enable the comparison to chamber estimates over hourly time scales, gap-filling of CH<sub>4</sub> fluxes was performed using marginal distribution sampling method implemented in ReddyProcWeb online tool (<https://www.bgc-jena.mpg.de/bgi/index.php/Services/REddyProcWeb>) (described in detail in Wutzler et al. (2018)).

MATLAB (ver. 2018a–b, Mathworks Inc., Natick, MA, USA) was used for all the eddy fluxes data analysis.

#### 2.7. Ancillary measurements

Air temperature and relative humidity were measured within the canopy at 10 m height using the HC2A-S3 – Standard Meteo Probe / RS24T (Rotronic AG, Bassersdorf, Switzerland) and Campbell CR100 data logger (Campbell Scientific Inc., Logan, UT, USA).

Soil temperature (Campbell Scientific Inc.) and soil water content (SWC) sensors (ML3 ThetaProbe, Delta-T Devices, Burwell, Cambridge, UK) were installed at 0–10 cm soil depth close to the studied trees. Near-ground air temperature sensors were installed directly on the ground. During six campaigns from August to November 2017 composite topsoil samples were taken with a soil corer from a depth of 0–10 cm for physical and chemical analysis using standard method (APHA-AWWA-WEF, 2005). In the groundwater of piezometers installed close to each analysed tree, dissolved O<sub>2</sub> concentration was measured using a handheld YSI Professional Plus Multiparameter Water Quality Instrument with a Quatro field cable (YSI Incorporated, Yellow Springs, OH, USA).

#### 2.8. Analysis of eddy covariance CH<sub>4</sub> data from global network

Worldwide, the network of research stations measuring CH<sub>4</sub> fluxes from ecosystems using the EC method is rapidly increasing. Most of the sites are included in FLUXNET, AMERIFLUX, ICOS and other regional networks (Knox et al., 2019). According to this source about 200 stations were listed where the EC method for CH<sub>4</sub> flux can be potentially used. We found 9 FLUXNET stations in forests from where the CH<sub>4</sub> flux data are available. Together with published papers, 21 data sources were available for the comparison with our results (Supplementary Table 2).

#### 2.9. Data analysis

R version 4.0.2 was used to examine, analyse and visualise the data. The significance level considered for all the tests was 0.05. The “akima” package version 0.6–2.1 was used to create interpolated contour plots representing a three-dimensional surface (Akima et al., 2016) by plotting soil temperature and SWC against soil CH<sub>4</sub> emissions as the independent variable. Linear regression models were fitted for soil temperature, SWC and soil CH<sub>4</sub> flux in Fig. 6. For Figs. 7, 9 and

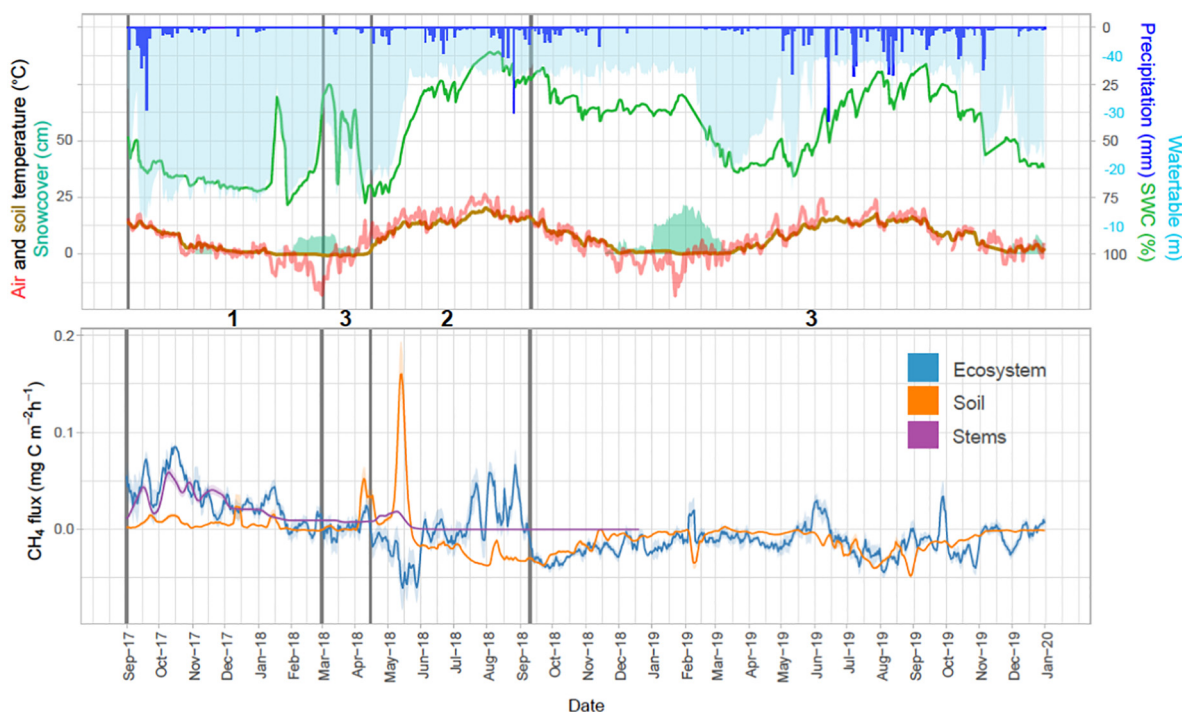


**Fig. 2.** Dynamics of environmental characteristics (above) and CH<sub>4</sub> fluxes at the soil ( $n = 105,000$ ), stem ( $n = 2145$ ) and ecosystem level (EC; below;  $n$  of gap-filled 1.5-h averaged values = 43,680) in the Agali grey alder forest during the Sept. 2017 – Dec. 2019 study period. Lines of CH<sub>4</sub> fluxes denote 5-day median values, the shaded area shows 25th and 75th percentiles. Periods of interest (borders marked with vertical lines): 1 - wet (2017-09-01 ... 2018-02-28), 2 - dry (2018-04-15... 2018-09-10), and 3 - the rest (2018-03-01...2018-04-14 and 2018-09-11...2019-12-31).

supplementary Fig. 4, a workflow for the nonlinear regression analysis was used (Archontoulis and Miguez, 2015) and regression models were fitted in R using functions `nls` or `loess`.

Based on high fluxes of CH<sub>4</sub> (both emission and consumption), and dynamics of SWC and near-ground air temperature, we identified three periods of interest (see numbers in Fig. 2): 1 - wet (2017-09-01 ... 2018-02-28), 2 - dry (2018-04-15... 2018-09-10), and 3 - the rest of the study (2018-03-01...2018-04-14 and 2018-09-11...2019-12-31).

### 3. Results

#### 3.1. General proportion of fluxes and CH<sub>4</sub> budget

CH<sub>4</sub> fluxes varied remarkably during the study (Fig. 2), displaying patterns that we divided into two periods of interest: wet and dry (Fig. 2). Average CH<sub>4</sub> fluxes from the soil varied from  $-68$  to  $210 \mu\text{g CH}_4\text{-C m}^{-2} \text{h}^{-1}$  and from tree stems  $-1.6$  to  $60 \mu\text{g CH}_4\text{-C m}^{-2} \text{h}^{-1}$  (units for both soil and stem are per ground area), being the highest during the wet period and the onset of dry period whereas the dry period was characterised with low CH<sub>4</sub> fluxes from both soil and stems (Fig. 2).

During the wet period, average  $\pm$  standard error (SE) CH<sub>4</sub> stem fluxes ( $224.4 \pm 6.3 \text{ mg CH}_4\text{-C m}^{-2} \text{yr}^{-1}$ ) contributed 83% of CH<sub>4</sub> measured above the canopy by EC technique (Table 1; Fig. 2), and ecosystem-level emissions were nearly equal to the sum of soil and stem emissions (Table 1). Consequently, during the whole year from

September 2017 to September 2018, the cumulative stem CH<sub>4</sub> flux was following the ecosystem-level measured cumulative flux curve, exceeding the soil flux negative value at the end of the period (Fig. 3a). In the dry period, average soil CH<sub>4</sub> flux was negative, however in the beginning of the period both soil and stems emitted CH<sub>4</sub> quite remarkably (up to 30 and 40  $\mu\text{g CH}_4\text{-C m}^{-2} \text{h}^{-1}$  on 5-days average, respectively; Fig. 3a, Supplementary Fig. 2). However, throughout the rest of dry period the soil CH<sub>4</sub> flux was negative and the stem emission close to zero (Fig. 2). A significant difference between the EC fluxes and the sum of soil and stem fluxes during the dry period was most likely caused by the emission from the canopy (Fig. 3b).

The EC measurements showed the forest was a slight annual sink of CH<sub>4</sub> across the whole study period ( $-53.6 \pm 3.4 \text{ mg CH}_4\text{-C m}^{-2} \text{yr}^{-1}$ ; Table 1).

Comparison of different years of the study demonstrates significance differences (Supplementary Table 3; Fig. 2): wet period with high soil and stem CH<sub>4</sub> fluxes at the end of 2017, significant drought period with fluctuating soil and ecosystem level fluxes CH<sub>4</sub> fluxes in 2018, and the rest of the study with relatively low soil and EC fluxes in 2019.

The main environmental factor determining CH<sub>4</sub> fluxes from all compartments was the soil water content which showed a strong positive correlation between the soil, tree stem and ecosystem-level fluxes; the Spearman's  $\rho$  correlations were 0.82, 0.75, and 0.33, respectively (Fig. 4). Soil temperature was the second most important environmental factor determining methane fluxes: Spearman's  $\rho$  values for soil and tree stem fluxes were  $-0.57$  and  $-0.48$ , respectively.

**Table 1**

Average  $\pm$  SE fluxes of CH<sub>4</sub> ( $\text{mg CH}_4\text{-C m}^{-2} \text{yr}^{-1}$ ) from all sources during the periods of interest and the whole study. See breakdown of periods in Fig. 2.

Source	Wet period (1)	Dry period (2)	Rest of the study (3)	Whole study
Soil	$48.0 \pm 4.6$	$-77.2 \pm 17.4$	$-82.2 \pm 2.6$	$-53.6 \pm 3.4$
Stems	$224.4 \pm 6.3$	$20.8 \pm 1.7$	$29.6 \pm 1.6$	$101.6 \pm 2.8^a$
Ecosystem (EC)	$270.1 \pm 14.8$	$4.0 \pm 2.6$	$-108.6 \pm 6.6$	$-24.0 \pm 6.7$

<sup>a</sup> Measured for the period of 487 days (from 2017 to 09-01 to 2018-12-31).

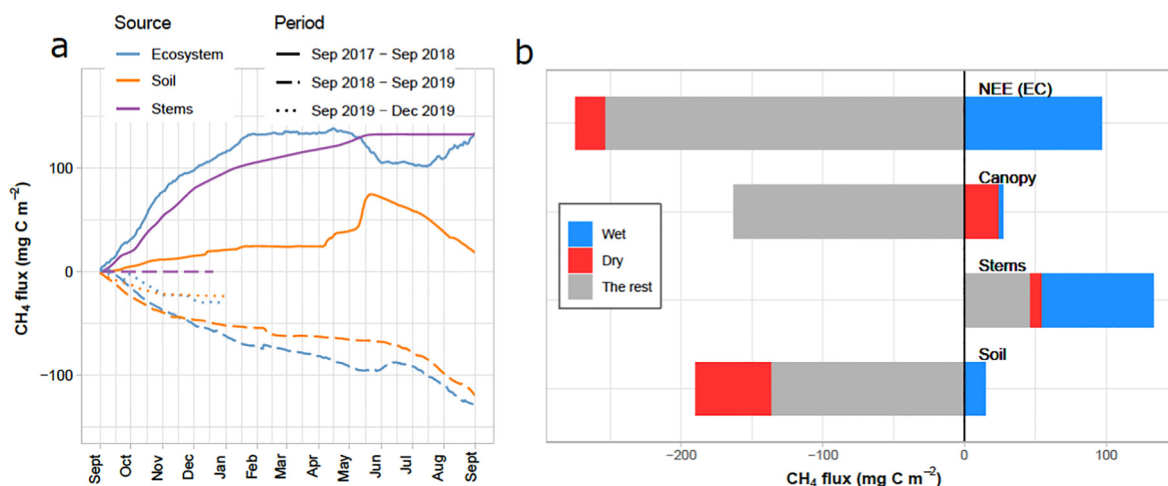


**Fig. 3.** Cumulative CH<sub>4</sub> fluxes from the soil, stems and ecosystem (eddy covariance above the canopies). (a) Fluxes during two full years (Sept. 2017–Sept. 2019) and one half-year (Sept.–Dec. 2019). Notice that the stem fluxes have been measured from Sept. 2017 to Dec. 2018 only. (b) The proportion of different CH<sub>4</sub> sources and sinks in the wet and dry period and over the whole study. Canopy flux was calculated as a difference between the eddy covariance (EC) fluxes, and the sum of soil and stem fluxes. NEE – net ecosystem exchange.

Throughout the whole study, tree stem CH<sub>4</sub> flux showed a significant positive Spearman's  $\rho$  correlation with ecosystem-level fluxes (Fig. 4), whereas during the wet period the correlation was stronger (Figs. 3a and 4). There was no significant correlation between the ecosystem-level fluxes and either air or soil temperature. Likewise, precipitation did not correlate with any of the CH<sub>4</sub> flux categories analysed. There was a strong positive Spearman's  $\rho$  correlation between the air and soil temperatures as expected but also a negative correlation between the soil temperature and soil water content ( $\rho = -0.56$ ; Fig. 4). At low but significant Spearman's  $\rho$  correlation values ( $\rho < 0.5$ ) we were cautious interpreting these results.

### 3.2. Soil fluxes

CH<sub>4</sub> fluxes varied from  $-61$  to  $210 \mu\text{g CH}_4\text{-C m}^{-2} \text{h}^{-1}$ . The heatmap in Supplementary Fig. 2 presents spatial and temporal variation of these values, showing that across the whole study period, no remarkable differences between the values measured in individual chambers were observed. However, chambers 2, 7, and 9 located in lower positions (10–15 cm from the average soil surface) showed somewhat higher values. Throughout the whole study soils were net consumers of methane (Fig. 5) with an average flux of  $-14.3 \pm 0.6 \mu\text{g CH}_4\text{-C m}^{-2} \text{h}^{-1}$  (Table 1). The temporal pattern of soil CH<sub>4</sub> fluxes showed seasonal variation, being remarkably higher during the wet period from September 2017 to February 2018 (average flux about  $45 \mu\text{g CH}_4\text{-C m}^{-2} \text{h}^{-1}$ ) as well as in winter 2018/2019 and late autumn 2019 (Fig. 5). The highest average flux values ( $60 \mu\text{g CH}_4\text{-C m}^{-2} \text{h}^{-1}$ ) were observed in a few days in the beginning of dry period in May 2018 (Fig. 2). During the wet period, a majority (>90%) of individual chambers showed daily average flux  $>0 \text{ mg CH}_4\text{-C m}^{-2} \text{h}^{-1}$  (Supplementary Fig. 2). The autumn (September–October) soil CH<sub>4</sub> fluxes were significantly higher in 2017 than those in following autumns (Fig. 5). This was caused by higher SWC in autumn 2017 (Fig. 2).

In most months during the whole study, differences between the daytime and nighttime CH<sub>4</sub> soil fluxes were not significant. At the beginning of the dry period (April–May 2018), somewhat higher fluxes in daytime were measured but these differences were not significant either (Supplementary Fig. 3).

The soil CH<sub>4</sub> flux was primarily determined by the soil water content and soil temperature (Fig. 6). Most emissions occurred under relatively high SWC ( $0.6\text{--}0.75 \text{ m}^3 \text{m}^{-3}$ ) whereas higher peaks were measured below  $14^\circ\text{C}$  and SWC range  $0.4\text{--}0.6 \text{ m}^3 \text{m}^{-3}$ , and in freezing-thawing conditions ( $-1$  to  $1.5^\circ\text{C}$  at SWC range  $0.35\text{--}0.75 \text{ m}^3 \text{m}^{-3}$ ; Fig. 6a).

However, the monthly average values from the freeze-thaw period in February 2019 did not show any remarkable increase in soil CH<sub>4</sub> fluxes (Figs. 2; 5; Supplementary Fig. 2).

The linear regression model of soil temperature and CH<sub>4</sub> fluxes showed a significant negative relationship ( $R^2 = 0.12$ ,  $p < 0.001$ ) although the above-mentioned peaks at lower ( $-1$  to  $1.5^\circ\text{C}$ ) and higher ( $13\text{--}14^\circ\text{C}$ ) temperature values were noticeable (Fig. 6b). According to the linear regression model of SWC and CH<sub>4</sub> fluxes, this relationship was positive ( $R^2 = 0.33$ ,  $p < 0.001$ ). Here, remarkably higher values of CH<sub>4</sub> flux were measured at the SWC range  $0.4\text{--}0.6 \text{ m}^3 \text{m}^{-3}$  (Fig. 6c). A non-linear curve with an optimal SWC range was obtained by a generalised additive model linking daily CH<sub>4</sub> fluxes from soil with SWC ( $R^2 = 0.29$ ,  $p < 0.001$ ; Supplementary Fig. 4).

### 3.3. Stem fluxes

CH<sub>4</sub> stem fluxes were the highest during the wet period and the onset of dry period (April 2018) reaching  $60 \mu\text{g CH}_4\text{-C m}^{-2} \text{h}^{-1}$  (calculated per m<sup>2</sup> of forest ground). CH<sub>4</sub> consumption by the stems was negligible. Median values of stem fluxes from the lowest parts of tree stems (10 cm from ground) were remarkably higher than those from the 80 and 170 cm ( $7.8$ ,  $3.0$  and  $1.0 \mu\text{g CH}_4\text{-C m}^{-2} \text{h}^{-1}$ , respectively).

For all the stem height sections we found a negative correlation between the dissolved oxygen concentration in groundwater and the CH<sub>4</sub> stem flux.

No significant differences between the daytime and nighttime CH<sub>4</sub> fluxes from tree stems were found ( $p > 0.05$ ).

A significant positive correlation (Spearman's  $\rho = 0.74$ ) was found between the soil and tree stem methane fluxes (Fig. 4).

### 3.4. Ecosystem fluxes (eddy covariance)

The average ecosystem-level CH<sub>4</sub> flux from the grey alder forest for the whole study was  $-0.07 \text{ mg CH}_4\text{-C m}^{-2} \text{d}^{-1}$  whereas weekly average CH<sub>4</sub> fluxes varied between  $-2.4$  and  $3.1 \text{ mg CH}_4\text{-C m}^{-2} \text{d}^{-1}$ ; Fig. 8). In wet period and following spring in 2018 the forest varied from a weak sink of CH<sub>4</sub> to a source, with weekly averages of  $-0.05$  to  $3.1 \text{ mg CH}_4\text{-C m}^{-2} \text{d}^{-1}$ . During the dry period largest fluctuations in CH<sub>4</sub> fluxes were observed, from consumption (down to  $-2.3 \text{ mg CH}_4\text{-C m}^{-2} \text{d}^{-1}$ ) in the beginning of the period to high emission (up to  $1.0\text{--}1.2 \text{ mg CH}_4\text{-C m}^{-2} \text{d}^{-1}$ ) at the second part of the period (Figs. 2 and 8). The latter has been considered as the heatwave (see Krasnova et al., 2022) lasting from July until mid-September 2018 and causing a

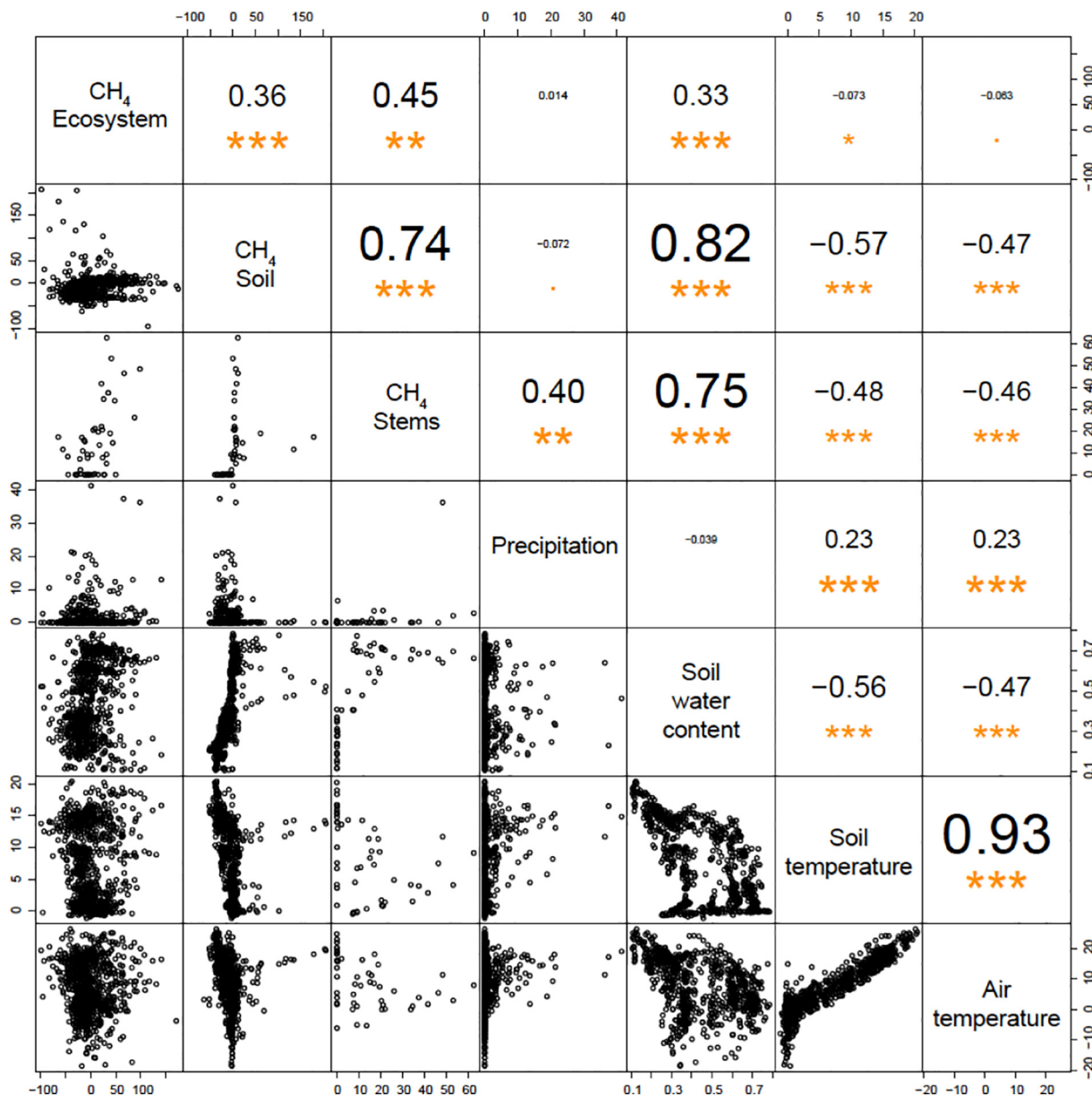


Fig. 4. Correlogram of Spearman's rank correlation coefficients ( $\rho$ ) between the soil, stem, and ecosystem (EC) CH<sub>4</sub> fluxes and key environmental factors.  $p$  values: \* -  $<0.05$ , \*\* -  $<0.01$ , \*\*\* -  $<0.001$ , \*\*\*\* -  $<0.0001$ . Units for parameters: CH<sub>4</sub> flux -  $\mu\text{g C m}^{-2} \text{h}^{-1}$ , precipitation -  $\text{mm d}^{-1}$ , soil water content -  $\text{m}^3 \text{m}^{-3}$ ; soil and air temperature -  $^{\circ}\text{C}$ .

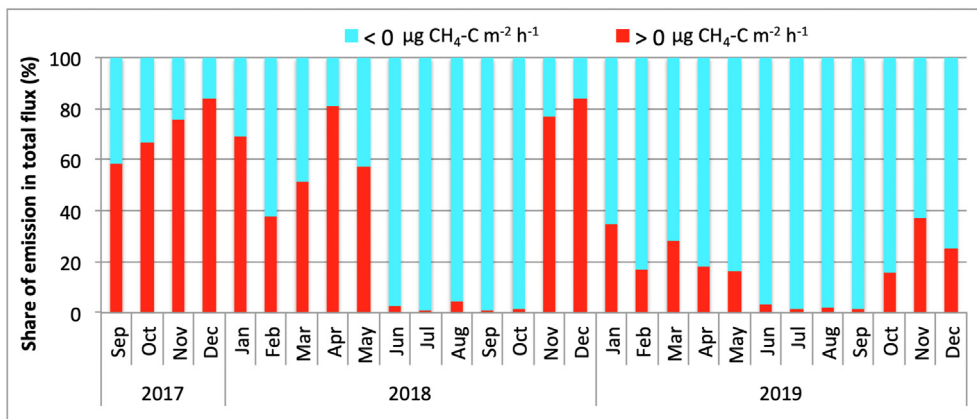
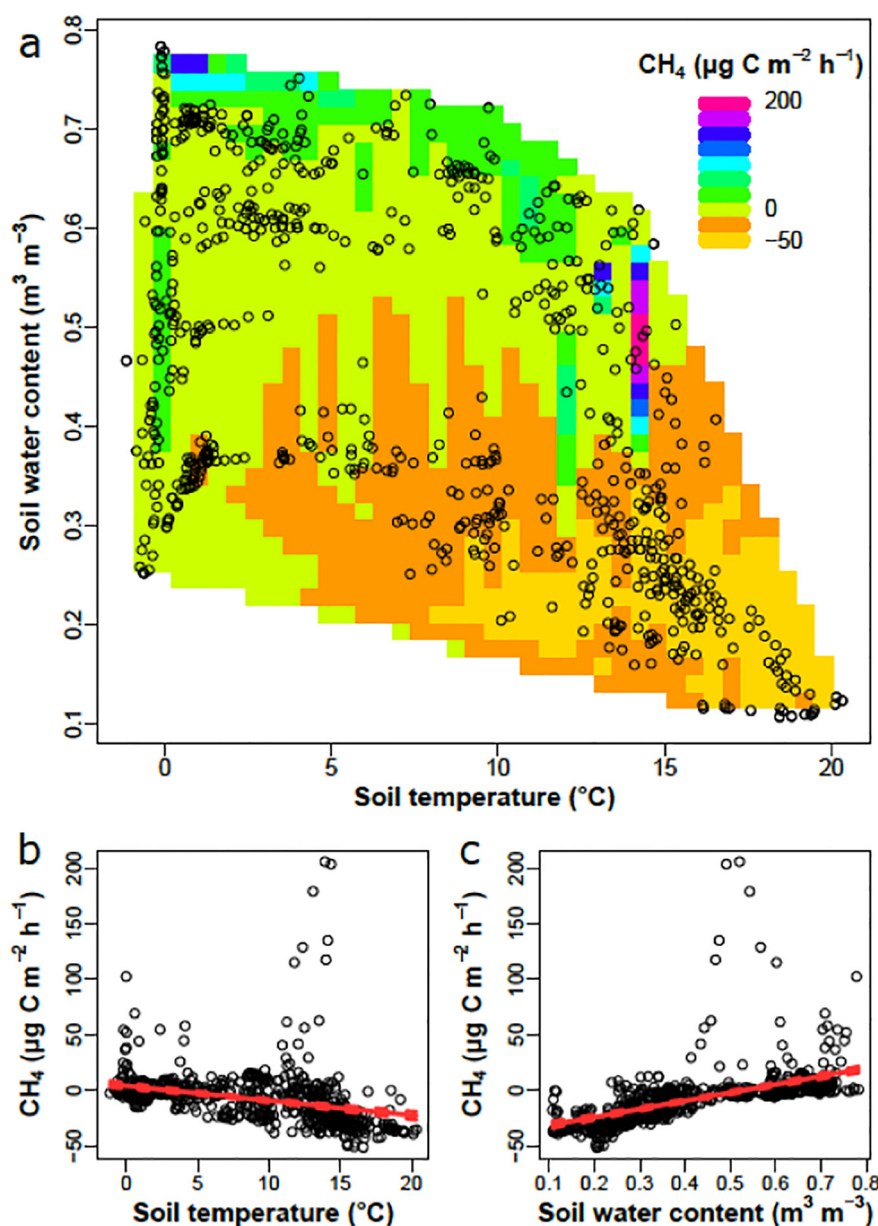


Fig. 5. Temporal pattern of soil CH<sub>4</sub> fluxes. A value of "0" separates consumption ("-" values) from emission ("+" values). Maximum possible number of measurements per month after quality check was between 228 and 372.





**Fig. 6.** Relationships between soil temperature, soil water content (SWC) and soil CH<sub>4</sub> flux over the whole study period. (a) Contour plot showing relationships between soil temperature, SWC and CH<sub>4</sub> fluxes ( $n = 755$ ). Using linear fitted regression, the variability of the CH<sub>4</sub> fluxes ( $R^2 = 0.33$ ,  $n = 755$ ) were determined mainly by soil moisture ( $p < 0.001$ ) and less by soil temperature ( $p > 0.05$ ). (b) Regression curve of soil temperature vs CH<sub>4</sub> flux. Linear fitted regression of soil temperature (ST) and CH<sub>4</sub> flux ( $R^2 = 0.12$ ,  $p < 0.001$ ,  $n = 756$ ).  $CH_4 = 4.11 + (-1.33) \times ST$ . (c) Regression curve of SWC vs CH<sub>4</sub> fluxes. Linear fitted regression of SWC and CH<sub>4</sub> flux ( $R^2 = 0.33$ ,  $p < 0.001$ ,  $n = 757$ ).  $CH_4 = -38.82 + 73.61 \times SWC$ . The dashed red lines represent 95% confidence intervals for the regression line. (For interpretation of the references to colour in this figure legend, the reader is referred to the web version of this article.)

remarkable consumption in soil but an unexpected short-lived emission from the whole ecosystem (Fig. 2). During the rest of the study period slight CH<sub>4</sub> consumption prevailed whereas in the freeze-thaw period in February 2019 slight increase in CH<sub>4</sub> emission was measured. Among the EC data about 25% were gap-filled (Fig. 8).

During the growing season (April–October) eddy covariance CH<sub>4</sub> fluxes showed a clear dependence on soil water content with the highest fluxes at a SWC value of  $0.7 \text{ m}^3 \text{ m}^{-3}$  (Supplementary Fig. 5).

A literature analysis of eddy covariance CH<sub>4</sub> measurements across forest ecosystems in different climate conditions showed that in regions with average annual air temperature  $< 10 \text{ }^\circ\text{C}$  (non-tropical areas mainly) the temperature dependence of CH<sub>4</sub> fluxes is unclear (Supplementary Table 2). In tropical regions ( $> 20 \text{ }^\circ\text{C}$ ) a rapid increase in CH<sub>4</sub> emission with air temperature can be observed (Fig. 9).

#### 4. Discussion

Due to the strong CH<sub>4</sub> oxidation capacity of soils, upland forests and some drained lowland forests are generally net CH<sub>4</sub> sinks (Dutaur and Verchot, 2007; Feng et al., 2020). This was also the case in our riparian forest, which was a minor net ecosystem-level sink of CH<sub>4</sub> (annual average  $-0.24 \text{ kg CH}_4\text{-C ha}^{-1} \text{ y}^{-1}$ ). Like our study, most of investigations highlighted soil water content as the leading determinant for all CH<sub>4</sub> fluxes from forest ecosystems (Covey and Megonigal, 2019; Feng et al., 2020). Riparian forests such as our study area are in the transitional zone between upland and wetland forests where environmental conditions typical for both forest types are combined (Flanagan et al., 2020). In our riparian forest soil CH<sub>4</sub> flux varied from net consumption to net emission (from  $-61$  to  $210 \text{ } \mu\text{g CH}_4\text{-C}$

$\text{m}^{-2} \text{h}^{-1}$ ; Table 1; Fig. 5; Supplementary Fig. 2) and followed the temporal dynamics of SWC (Figs. 2 & 5).

However, relatively recent findings on  $\text{CH}_4$  exchange between the trees and the atmosphere demonstrate that  $\text{CH}_4$  emission from tree stems and other biotic surfaces in forest ecosystems might decrease their sink strength, even becoming ecosystem-scale net  $\text{CH}_4$  sources during certain periods (Pitz and Megonigal, 2017; Covey and Megonigal, 2019; Feng et al., 2020). In contrast to some investigations, which emphasize the  $\text{CH}_4$  production directly within stems (Barba et al., 2019; Yip et al., 2019; Barba et al., 2021), our results show that methane has been formed within the soil and transported by trees to the atmosphere. This assumption is supported by the fact that the lowest parts of stems emit significantly more methane than the higher sections and  $\text{CH}_4$  stem flux is negatively correlated with the dissolved oxygen concentration in groundwater (Fig. 7).

In our study the ecosystem was a net  $\text{CH}_4$  source only during the wet conditions with high SWC and groundwater table when the stems emitted more than the soil, and the stem fluxes constituted 81% of the ecosystem-level fluxes (Figs. 2 and 3). For the entire 2.5-year study period ecosystem flux was still slightly negative indicating that this riparian alder forest was a net sink of  $\text{CH}_4$ . In a similar riparian ecosystem, a cottonwood forest in Alberta, Canada, the stem  $\text{CH}_4$  emissions offset 86% of the soil uptake (Flanagan et al., 2020).

Shoemaker et al. (2014) demonstrates that due to the changes in late summer water balance, a temperate coniferous forest in Maine, USA changed from an annual  $\text{CH}_4$  source to sink. These changes are typical for temperate forest ecosystems where weather conditions change seasonally (Dutaur and Verchot, 2007; Covey and Megonigal, 2019; Knox et al., 2019) and in the tropics at constantly high air and soil temperature where the seasonality occurs mostly on the basis of precipitation regime (Sakabe et al., 2018; Dalmagro et al., 2019; Griffis et al., 2020).

The temporal variations of  $\text{CH}_4$  fluxes in forests can be characterised as short-term (diurnal), synoptic (depending on weather conditions), and seasonal (long-term) changes (Vargas and Barba, 2019). In our study, some diurnal pattern was observed only for ecosystem-level  $\text{CH}_4$  fluxes and only during the wet period growing season (September 2017, May–July 2018, and May–September 2019) when the daytime EC fluxes exceeded the nighttime fluxes, whereas in the dormant season, the difference was not significant (Supplementary Fig. 6). Likewise, Dalmagro et al. (2019) found, that in a tropical forested wetland in Pantanal, Brazil during periods of higher water table depth (anaerobic soil), daytime fluxes were clearly higher than nighttime. In contrast, Sakabe et al. (2018) found significantly higher nighttime  $\text{CH}_4$  from the EC measurements in a tropical peatland forest in Indonesia.

Regarding the soil and stem  $\text{CH}_4$  fluxes, we could not find any clear diurnal pattern. In contrast some other studies have shown that daytime  $\text{CH}_4$  fluxes from tree stems exceed the nighttime fluxes (Pangala et al., 2014; Megonigal et al., 2019).

There is evidence that cryptogamic cover (lichens, mosses, algae) on tree stems can emit methane (Lenhart et al., 2015). However, our initial comparison of stem chambers with cryptogams and those without could not find any remarkable differences in  $\text{CH}_4$  flux. Nevertheless, the role of microorganisms on the bark and within the stems remains unclear and only a few recent studies shed light on it (Yip et al., 2019; Jeffrey et al., 2021; Putkinen et al., 2021).

Our study showed a clear dependence of  $\text{CH}_4$  soil fluxes on soil water content (Fig. 6). Methanogenesis in soil requires anaerobic conditions which are supported by high water table (Le Mer and Roger, 2001). Soil and air temperature also emerged as significant factors controlling methane fluxes (Figs. 6 and 9). However, the role of freezing-thawing effect on  $\text{CH}_4$  soil fluxes was not obvious. We could see some increase in  $\text{CH}_4$  fluxes at around-zero soil temperature in February 2019. It could be related to the impact of snowmelt water, which filled the soil pores and created short-term peaks in  $\text{CH}_4$  fluxes, still being insignificant for the annual  $\text{CH}_4$  budget of this forest (Fig. 6). Likewise, Pihlatie et al. (2010) did not find any freeze-thaw effect in  $\text{CH}_4$  fluxes from a peatland forest soil. Under analogous conditions in drained peatland forests high  $\text{N}_2\text{O}$  but no  $\text{CH}_4$  fluxes were measured (Virus et al., 2020). In February–March 2018, snow cover of 15–25 cm likely decreased the  $\text{CH}_4$  soil flux (Fig. 2) as observed by Borken et al. (2006) observed a similar effect of snow cover on  $\text{CH}_4$  fluxes.

We were able to demonstrate a clear effect of soil water content (SWC) on both  $\text{CH}_4$  fluxes from the tree stem and ecosystem levels. We found a significant positive correlation (Spearman's  $\rho = 0.74$ ) between the soil and tree stem  $\text{CH}_4$  fluxes (Fig. 4). There was an optimal SWC range at  $0.6\text{--}0.7 \text{ m}^3 \text{ m}^{-3}$  at which the  $\text{CH}_4$  stem fluxes were the highest whereas the optimum for soil  $\text{CH}_4$  fluxes occurs at a SWC range of  $0.4\text{--}0.5 \text{ m}^3 \text{ m}^{-3}$  (Supplementary Fig. 4). This refers to a likely reciprocal alteration of the role of the soil and tree stems, which depends on the soil water conditions. It can be that the stem flux is more sensitive to SWC changes whereas soil emissions peak at a relatively high SWC values, especially during the rapid decrease of SWC during the onset of dry period in May 2018 (Fig. 2). Likewise, SWC range from  $0.45$  to  $0.65 \text{ m}^3 \text{ m}^{-3}$  appears to be optimal for ecosystem-level  $\text{CH}_4$  fluxes (Supplementary Fig. 5).

Soil temperature showed a negative Spearman's  $\rho$  correlation with both soil and stem  $\text{CH}_4$  fluxes, most likely due to the negative correlation between the soil water content and temperature (Fig. 4).

Regarding the budget of  $\text{CH}_4$  in riparian forests we were able to demonstrate the role of the canopy in situ. During the dry period the canopy is a net  $\text{CH}_4$  source, emitted about 20% of the  $\text{CH}_4$  from all sources during this time periods (Figs. 2 & 3b; without accounting for the gap-filled  $\text{CH}_4$  fluxes; Fig. 8). The dry period coincided with a heat wave in June–July 2018 Krasnova et al., 2022 and potentially high fluxes of UV-B radiation (unpublished data from the nearby SMEAR Estonia station, see also Noe et al., 2015) that can be interpreted as evidence of the abiotic aerobic production of  $\text{CH}_4$  from leaves (Keppler et al., 2006;

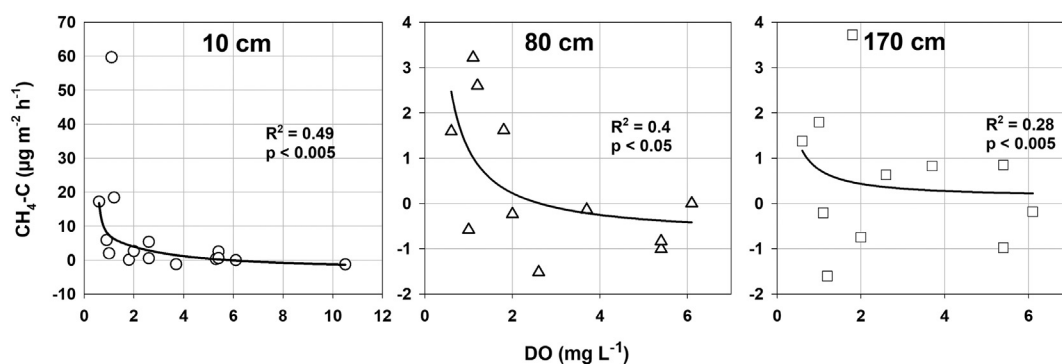
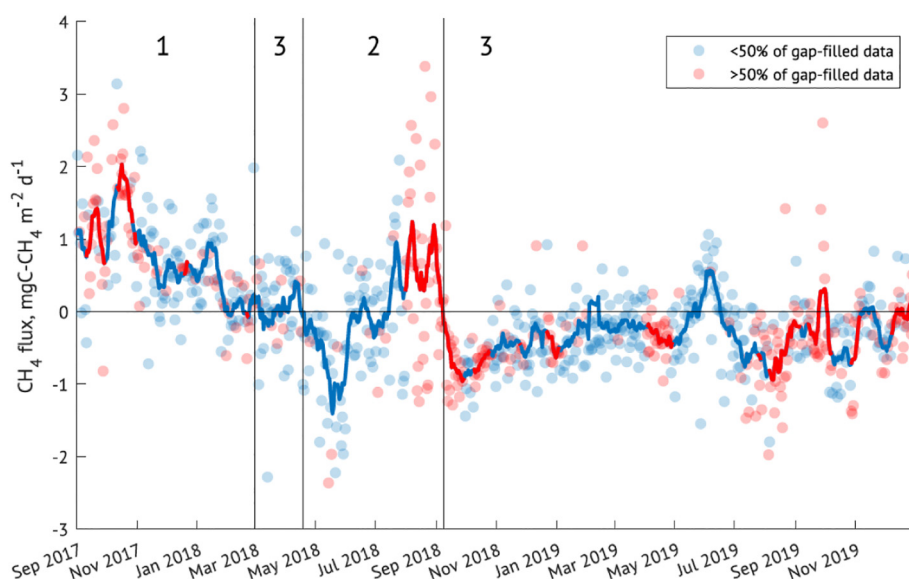


Fig. 7. Relationships between the groundwater dissolved oxygen (DO) concentration and stem  $\text{CH}_4$  flux at the heights of 10 ( $n = 15$ ), 80 ( $n = 11$ ) and 170 cm ( $n = 11$ ). The curves show non-linear regression line based on third order polynomial equations.



**Fig. 8.** Seasonal cycle of ecosystem  $\text{CH}_4$  flux measured with QCLAS in eddy tower. Flux values above zero indicate emission while below the zero mean consumption of  $\text{CH}_4$ . The markers denote daily total values, the fitted line is a seven-day running mean. The periods marked with red colour represent time intervals with gap-filled data (MDS-method) exceeding 50%. Periods of interest: 1 - wet (2017-09-01 ... 2018-03-01), 2 - dry (2018-04-15... 2018-09-10). (For interpretation of the references to colour in this figure legend, the reader is referred to the web version of this article.)

Vigano et al., 2008; Covey and Megonigal, 2019). Likewise, Mikkelsen et al. (2012) have demonstrated the  $\text{CH}_4$  release from forest canopy using profile measurements at different heights. During the rest of our study (outside of wet and dry periods), the influence of the canopy on the forest  $\text{CH}_4$  budget was large, but in the opposite direction as a net  $\text{CH}_4$  sink. This can be related to microbial  $\text{CH}_4$  consumption within the canopy as proposed by Putkinen et al. (2021), or to several meteorological and microclimatological conditions within the canopy (see Mikkelsen et al., 2012). In addition, advective transport and storage fluxes of methane may play a role in this process, which emphasizes the

need for further profile measurements within the canopy (Rebmann et al., 2018).

The results of our long-term study show that the role of riparian alder forests as net  $\text{CH}_4$  sinks accrues from a complex array of soil and plant processes that both produce and consume this powerful greenhouse gas. These processes respond to environmental variation somewhat independently such that the both the source and sink strength significantly vary over time, including occasionally switching the forest from a net  $\text{CH}_4$  sink to a net source. Thus, the buffering capacity of this riparian alder forest (and certainly other riparian forests) on the atmospheric  $\text{CH}_4$  budget is high and responds to perturbations such as global climate change. This complexity makes it challenging to forecast without building a deeper understanding of  $\text{CH}_4$  cycling processes in forests generally.

For better understanding of carbon budgets of riparian forests, we need long-term, high-frequency measurements of fluxes from the soil and tree stems in combination with ecosystem-level EC measurements. Likewise, the role of canopy in forest ecosystem  $\text{CH}_4$  budgets needs to be better understood and therefore, canopy flux measurements with shoot chambers and gradient analysis of  $\text{CH}_4$  concentration within the canopy are strongly recommended for further studies. The identification of microorganisms and biogeochemical pathways associated with  $\text{CH}_4$  production and consumption is another future challenge.

## 5. Conclusions

Our study showed that riparian deciduous forests growing on gleysols in a transitional zone from mineral to organic soils with relatively high groundwater table is a weak long-term  $\text{CH}_4$  sink. Thus, the first hypothesis that this riparian forest ecosystem is a net  $\text{CH}_4$  sink was supported. However, there was a significant difference in  $\text{CH}_4$  fluxes between the wet and dry periods, showing differences in the contributions of soils, stems, and canopy processes to ecosystem-level (EC) fluxes. During the wet period in autumn and early winter 2017/2018, 81% of ecosystem  $\text{CH}_4$  emissions was emitted by tree stems and the sum of soil and stem fluxes was similar to the ecosystem (EC) fluxes indicating the canopy was neither a net  $\text{CH}_4$  source nor sink. In the dry period (late spring and summer 2018),  $\text{CH}_4$  was consumed at the soil surface and emitted, most likely, from the canopy, while the stem emissions were very low. Soil water content was the most

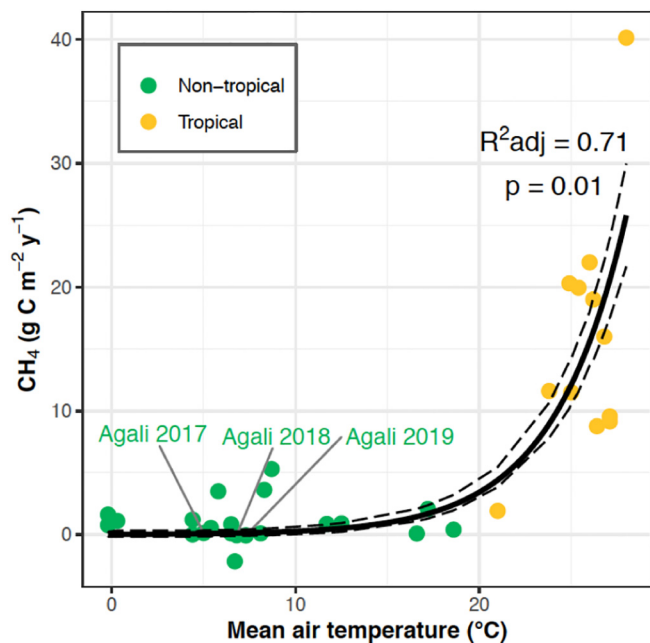


**Fig. 9.** Relationship between mean annual air temperature and the EC-measured mean annual  $\text{CH}_4$  emission in forest ecosystems across the climate zones. Dashed line shows 95% confidence limits. Values for the Agali study site in our research for 2017 (Sept-Dec), 2018 and 2019 are indicated by green symbols. See Supplementary Table 2 for details. (For interpretation of the references to colour in this figure legend, the reader is referred to the web version of this article.)

important environmental factor controlling both soil and stem fluxes. Likewise, there was a significant positive correlation between soil moisture and EC CH<sub>4</sub> fluxes. Accordingly, a positive correlation between soil and stem fluxes was observed that supports our third and fourth hypotheses. Soil temperature showed a negative correlation with both soil and stem CH<sub>4</sub> fluxes, most likely due to the negative correlation between the soil water content and temperature. Quite surprisingly, we found an optimum SWC value that differed for soil fluxes versus stem CH<sub>4</sub> fluxes.

### CRediT authorship contribution statement

Ülo Mander, Kaido Soosaar, Katerina Machacova and Ülo Niinemets designed this study; Ülo Mander, Kaido Soosaar, Alisa Krasnova, Jaan Pärn, Mikko Espenberg, Jordi Escuer-Gatius, Thomas Schindler, J. Patrick Megonigal and Mari Pihlatie wrote the paper; Thomas Schindler, Martin Maddison, Kaido Soosaar and Ülo Mander conducted the field work, Ülo Mander, Kaido Soosaar Alisa Krasnova, Mikko Espenberg, Jordi Escuer-Gatius, Kuno Kasak, Reti Ranniku and Katerina Machacova carried out data checks and analysis, and all authors commented on the paper.

### Funding

This study was supported by the Ministry of Education and Science of Estonia (SF0180127s08 grant), the Estonian Research Council (IUT2-16, PRG-352, and MOBERC20), the Czech Science Foundation (17-18112Y), SustES - Adaptation strategies for sustainable ecosystem services and food security under adverse environmental conditions (CZ.02.1.01/0.0/0.0/16\_019/0000797), the Ministry of Education, Youth and Sports of Czech Republic within the National Sustainability Program I (NPU I, grant number LO1415), the EU through the European Regional Development Fund (ENVIRON and EcolChange Centres of Excellence, Estonia, and MOBTP101 returning researcher grant by the Mobilias Plus programme), the European Social Fund (Doctoral School of Earth Sciences and Ecology). This work was also supported by Academy of Finland (294088, 288494), from the European Research Council (ERC) under the European Union's Horizon 2020 research and innovation programme under grant agreement No [757695], and a Department of Energy (DOE) grant to JPM (DE-SC0008165).

### Declaration of competing interest

The authors declare that they have no known competing financial interests or personal relationships that could have appeared to influence the work reported in this paper.

### Acknowledgements

We would like to thank Marek Jakubík, Dmitrii Krasnov, Dr. Gunnar Morozov, Mart Muhel, Dr. Alar Teemusk and Gert Veber for their technical support.

### Appendix A. Supplementary data

Supplementary data to this article can be found online at <https://doi.org/10.1016/j.scitotenv.2021.151723>.

### References

Abdalla, M., Hastings, A., Truu, J., Espenberg, M., Mander, Ü., Smith, P., 2016. Emissions of methane from northern peatlands: a review of management impacts and implications for future management options. *Ecol. Evol.* 6 (19), 7080–7102. <https://doi.org/10.1002/ece3.2469>.

Akima, H., Gebhardt, A., Petzold, T., Maechler, M., 2016. akima: Interpolation of irregularly and regularly spaced data. R Package Version 0.6-2.1. <https://cran.r-project.org/web/packages/akima/index.html>. (Accessed 8 June 2021).

APHA-AWWA-WEF, 2005. *Standard Methods for the Examination of Water and Wastewater*. 21th ed. American Public Health Organisation.

Archontoulis, S.V., Miguez, F.E., 2015. Nonlinear regression models and applications in agricultural research. *Agron. J.* 107 (2), 786–798. <https://doi.org/10.2134/agronj2012.0506>.

Barba, J., Bradford, M.A., Brewer, P.E., Bruhn, D., Covey, K., van Haren, J., et al., 2018. Methane emissions from tree stems: a new frontier in the global carbon cycle. *New Phytol.* 222, 18–28. <https://doi.org/10.1111/nph.15582>.

Barba, J., Poyatos, R., Vargas, R., 2019. Automated measurements of greenhouse gases fluxes from tree stems and soils: magnitudes, patterns and drivers. *Sci. Rep.* 9, 4005. <https://doi.org/10.1038/s41598-019-39663-8>.

Barba, J., Poyatos, R., Capocci, M., Vargas, R., 2021. Spatiotemporal variability and origin of CO<sub>2</sub> and CH<sub>4</sub> tree stem fluxes in an upland forest. *Glob. Change Biol.* 27, 4879–4893. <https://doi.org/10.1111/gcb.15783>.

Becker, H., Uri, V., Aosaar, J., Varik, M., Mander, Ü., Soosaar, K., et al., 2015. The effects of clear-cut on net nitrogen mineralization and nitrogen losses in a grey alder stand. *Ecol. Eng.* 85, 237–246. <https://doi.org/10.1016/j.ecoleng.2015.10.006>.

Borken, W., Davidson, E.A., Savage, K., Sundquist, E.T., Steudler, P., 2006. Effect of summer throughfall exclusion, summer drought, and winter snow cover on methane fluxes in a temperate forest soil. *Soil Biol. Biochem.* 38, 1388–1395. <https://doi.org/10.1016/j.soilbio.2005.10.011>.

Carter, M.S., Larsen, K.S., Emmett, B., Estiarte, M., Field, C., Leith, I.D., et al., 2012. Synthesizing greenhouse gas fluxes across nine European peatlands and shrublands – responses to climatic and environmental changes. *Biogeosciences* 9, 3739–3755.

Caudullo, G., Welk, E., San-Miguel-Ayanz, J., 2017. Chorological maps for the main European woody species. *Data in Brief*. 12, pp. 662–666. <https://doi.org/10.1016/j.dib.2017.05.007>.

Clerici, N., Weissteiner, C.J., Paracchini, M.L., Boschetti, L., Baraldi, A., Strobl, P., 2013. Pan-European distribution modelling of stream riparian zones based on multi-source earth observation data. *Ecol. Indic.* 24, 211–223. <https://doi.org/10.1016/j.ecolind.2012.06.002>.

Courtois, E.A., Stahl, C., Van den Berge, J., Brechet, L., Van Langenhove, L., Richter, A., et al., 2018. Spatial variation of soil CO<sub>2</sub>, CH<sub>4</sub> and N<sub>2</sub>O fluxes across topographical positions in tropical forests of the guiana shield. *Ecosystems* 21 (7), 1445–1458. <https://doi.org/10.1111/nph.15624>.

Covey, K.R., Megonigal, J.P., 2019. 222, 35–51. <https://doi.org/10.1111/nph.15624>.

Covey, K.R., Wood, S.A., Warren, R.J., Lee, X., Bradford, M.A., 2012. Elevated methane concentrations in trees of an upland forest. *Geophys. Res. Lett.* 39, L15705. <https://doi.org/10.1029/2012GL052361>.

Dalmagro, H.J., Zanella de Arruda, P.H., Vourlitis, G.L., Lathuillière, M.J., Nogueira, J.D.S., Couto, E.G., Johnson, M.S., 2019. Radiative forcing of methane fluxes offsets net carbon dioxide uptake for a tropical flooded forest. *Glob. Change Biol.* 25, 1967–1981. <https://doi.org/10.1111/gcb.14615>.

Del Grosso, S.J., Parton, W.J., Mosier, A.R., Ojima, D.S., Potter, C.S., Borken, W., et al., 2000. General CH<sub>4</sub> oxidation model and comparisons of CH<sub>4</sub> oxidation in natural and managed systems. *Glob. Biogeochem. Cy.* 14 (4), 999–1019. <https://doi.org/10.1029/1999GB001226>.

Dlugokencky, E.J., Nisbet, E.G., Fisher, R., Lowry, D., 2011. Global atmospheric methane: budget, changes and dangers. *Philos. Trans. R. Soc. A* 369, 2058–2072. <https://doi.org/10.1098/rsta.2010.0341>.

do Carmo, J.B., Keller, M., Dias, J.D., Camargo, P.B.D., Crill, P., 2006. A source of methane from upland forests in the Brazilian Amazon. *Geophys. Res. Lett.* 33 (4), L04809. <https://doi.org/10.1029/2005GL025436>.

Dutaur, L., Verchot, L.V., 2007. A global inventory of the soil CH<sub>4</sub> sink. *Glob. Biogeochem. Cy.* 21 (4), 1–9. <https://doi.org/10.1029/2006GB002734>.

Feng, H., Guo, J., Han, M., Wang, W., Peng, C., Jin, J., Song, X., Yu, S., 2020. A review of the mechanisms and controlling factors of methane dynamics in forest ecosystems. *For. Ecol. Manag.* 455, 117702. <https://doi.org/10.1016/j.foreco.2019.117702>.

Flanagan, L.B., Nikkel, D.J., Scherloski, L.M., Tkach, R.E., Smits, K.M., Selinger, B., Rood, S.B., 2020. Multiple processes contribute to methane emission in a riparian cottonwood forest ecosystem. *New Phytol.* 229, 1970–1982. <https://doi.org/10.1111/nph.16977>.

Foken, T., Göckede, M., Mauder, M., 2004. Post-field data quality control. In: Lee, X., Massman, W.J., Law, B.E. (Eds.), *Handbook of Micrometeorology: A Guide for Surface Flux Measurements*. Kluwer Academic, Dordrecht, pp. 181–208 Issue 1988.

Gauci, V., Gowing, D.J.G., Hornibrook, E.R.C., Davis, J.M., Dise, N.B., 2010. Woody stem methane emission in mature wetland alder trees. *Atmos. Environ.* 44 (1), 2157–2160. <https://doi.org/10.1016/j.atmosenv.2010.02.034>.

Griffis, T.J., Roman, D.T., Wood, J.D., Deventer, J., Fachin, L., Rengifo, J., et al., 2020. Hydro-meteorological sensitivities of net ecosystem carbon dioxide and methane exchange of an amazonian palm swamp peatland. *Agric. For. Meteorol.* 295, 108167. <https://doi.org/10.1016/j.agrformet.2020.108167>.

Große, W., Schröder, P., 1984. Oxygen supply of roots by gas transport in alder-trees. *Z. Naturforsch. C* 39, 1186–1188.

Han, M., Zhu, B., 2020. Changes in soil greenhouse gas fluxes by land use change from primary forest. *Glob. Change Biol.* 26 (4), 2656–2667. <https://doi.org/10.1111/gcb.14993>.

Hommelntenberg, J., Mauder, M., Dröslér, M., Heidbach, K., Werle, P., Schmid, H.P., 2014. Ecosystem scale methane fluxes in a natural temperate bog-pine forest in southern Germany. *Agric. For. Meteorol.* 198–199, 273–284. <https://doi.org/10.1016/j.agrformet.2014.08.017>.

IPCC, 2014. *Climate Change 2014: Mitigation of Climate Change*. Cambridge University Press <https://doi.org/10.1017/cbo9781107415416>.

Itoh, M., Ohte, N., Koba, K., 2008. Methane flux characteristics in forest soils under an east asian monsoon climate. *Soil Biol. Biochem.* 41 (2), 388–395. <https://doi.org/10.1016/j.soilbio.2008.12.003>.

Iwata, H., Harazono, Y., Ueyama, M., Sakabe, A., Nagano, H., Kosugi, Y., 2015. Methane exchange in a poorly-drained black spruce forest over permafrost observed using the



- ecosystems, and uncertainties in the global terrestrial sink. *Glob. Change Biol.* 6 (7), 791–803. <https://doi.org/10.1046/j.1365-2486.2000.00356.x>.
- Soosaar, K., Mander, Ü., Maddison, M., Kanal, A., Kull, A., Lõhmus, K., et al., 2011. Dynamics of gaseous nitrogen and carbon fluxes in riparian alder forests. *Ecol. Eng.* 37 (1), 40–53. <https://doi.org/10.1016/j.ecoleng.2010.07.025>.
- Sweeney, B.W., Bott, T.L., Jackson, J.K., Kaplan, L.A., Newbold, J.D., Standley, L.J., et al., 2004. Riparian deforestation, stream narrowing, and loss of stream ecosystem services. *Proc. Natl. Acad. Sci. U. S. A.* 101, 14132–14137. <https://doi.org/10.1073/pnas.0405895101>.
- Tan, L., Ge, Z., Zhou, X., Li, S., Li, X., Tang, J., 2020. Conversion of coastal wetlands, riparian wetlands, and peatlands increases greenhouse gas emissions: a global meta-analysis. *Glob. Change Biol.* 26 (3), 1638–1653. <https://doi.org/10.1111/gcb.14933>.
- Terazawa, K., Yamada, K., Ohno, Y., Sakata, T., Ishizuka, S., 2015. Spatial and temporal variability in methane emissions from tree stems of *Fraxinus mandshurica* in a cool-temperate floodplain forest. *Biogeochemistry* 123, 349–362. <https://doi.org/10.1007/s10533-015-0070-y>.
- Turetsky, M.R., Kotowska, A., Bubier, J., Dise, N.B., Crill, P., Hornibrook, E.R.C., et al., 2014. A synthesis of methane emissions from 71 northern, temperate, and subtropical wetlands. *Glob. Change Biol.* 20, 2183–2197. <https://doi.org/10.1111/gcb.12580>.
- Uri, V., Aosaar, J., Varik, M., Becker, H., Ligi, K., Padari, A., et al., 2014. The dynamics of biomass production, carbon and nitrogen accumulation in grey alder (*Alnus incana* (L.) Moench) chronosequence stands in Estonia. *Forest Ecol. Manag.* 327, 106–117. <https://doi.org/10.1016/j.foreco.2014.04.040>.
- Varep, E., 1964. The landscape regions of Estonia. *Publications on Geography IV. Acta et Comm.* 156. Universitatis Tartuensis, pp. 3–28.
- Vargas, R., Barba, J., 2019. Greenhouse gas fluxes from tree stems. *Trends Plant Sci.* 24, 296–299. <https://doi.org/10.1016/j.tplants.2019.02.005>.
- Vigano, I., van Weelden, H., Holzinger, R., Keppler, F., Röckmann, T., 2008. Effect of UV radiation and temperature on the emission of methane from plant biomass and structural components. *Biogeosciences* 5, 937–947. <https://doi.org/10.5194/bg-5-937-2008>.
- Viru, B., Veber, G., Jaagus, J., Kull, A., Maddison, M., Muhel, M., et al., 2020. Wintertime greenhouse gas fluxes from hemiboreal drained peatlands. *Atmosphere* 11, 731. <https://doi.org/10.3390/atmos11070731>.
- Wang, Z.-P., Han, S.-J., Li, H.-L., Deng, F.-D., Zheng, Y.-H., Liu, H.-F., et al., 2017. Methane production explained largely by water content in the heartwood of living trees in upland forests. *JGR Biogeosciences* 122, 2479–2489. <https://doi.org/10.1002/2017JG003991>.
- Wang, J.M., Murphy, J.G., Geddes, J.A., Winsborough, C.L., Basiliko, N., Thomas, S.C., 2013. Methane fluxes measured by eddy covariance and static chamber techniques at a temperate forest in Central Ontario, Canada. *Biogeosciences* 10, 4371–4382. <https://doi.org/10.5194/bg-10-4371-2013>.
- Warner, D.L., Villarreal, S., McWilliams, K., Inamdar, S., Vargas, R., 2017. Carbon dioxide and methane fluxes from tree stems, coarse woody debris, and soils in an upland temperate forest. *Ecosystems* 20 (6), 1205–1216. <https://doi.org/10.1007/s10021-016-0106-8>.
- Wong, G.X., Hirata, R., Hirano, T., Kiewa, F., Aeries, E.B., Musin, K.K., et al., 2018. Micrometeorological measurement of methane flux above a tropical peat swamp forest. *Agric. For. Meteorol.* 256–257, 353–361. <https://doi.org/10.1016/j.agrformet.2018.03.025>.
- Wutzler, T., Lucas-Moffat, A.L., Migliavacca, M., Knauer, J., Sickel, K., Sigut, L., et al., 2018. Basic and extensible post-processing of eddy covariance flux data with REddyProc. *Biogeosciences* 15 (16), 5015–5030. <https://doi.org/10.5194/bg-15-5015-2018>.
- Yip, D.Z., Veach, A.M., Yang, Z.K., Cregger, M.A., Schadt, C.W., 2019. Methanogenic archaea dominate mature hardwood habitats of eastern cottonwood (*Populus deltoides*). *New Phytol.* 222, 115–121. <https://doi.org/10.1111/nph.15346>.
- Yu, L., Huang, Y., Zhang, W., Li, T., Sun, W., 2017. Methane uptake in global forest and grassland soils from 1981 to 2010. *Sci. Total Environ.* 607–608, 1163–1172. <https://doi.org/10.1016/j.scitotenv.2017.07.082>.
- Zeikus, J.G., Ward, J.C., 1974. Methane formation in living trees: a microbial origin. *Science* 184, 1181–1183. <https://doi.org/10.1126/science.184.4142.1181>.